MALS commissioning observations of J1639+1127 and J2023-3655

(N. Gupta, P. Jagannathan)

May 22, 2020

1. Description of the target and observations

(For a quick summary see last section *Concluding remarks*)

Context: The first MALS commissioning observation using MeerKAT-64 and the 32K mode of the SKARAB correlator, focused on PKS1830-211. These observations which were carried out on December 19, 2019 led to successful detection of known HI 21-cm absorption at z=0.190 (observing frequency ~ 1191 MHz) and OH 18-cm absorption at z=0.885 (observing frequency ~ 853 MHz). These observations demonstrated the excellent spectral line capabilities of the telescope across the entire L-band (cf. report on PKS1830-211). But the spectral and continuum rms were found to be a factor 4 higher than the theoretically expected value. This was attributed to dynamic range issues due to extremely high flux density (~10 Jy) of the quasar. In order to test this it was decided to observe targets lower in flux density but still spanning the range relevant for MALS.

Targets and observations: The fields centered at J1639+1127 and J2023-3655 were observed on April 1, 2020 with MeerKAT-64 array using 59 antennas. The total integration time on each target is **~56 mins** (same as to be used for MALS L-band phase). For the observations, the total bandwidth of 856 MHz centered at 1283.9869 MHz was split into 32768 channels (frequency resolution = 26.123 kHz). The correlator dump time was 8 seconds and the data were acquired for all 4 polarization products, labelled XX, XY, YX and YY. J1331+3030 and J1939-6342 were observed for flux density and bandpass calibrations.

Target source	Position (J2000)	S(1.4 GHz)	Redshift	Gain calibrator
J1639+1127	16:39:56.35 +11:27:58.7	170 mJy	0.993	J1550+0527
J2023-3655	20:23:46.21 -36:55:21.2	436 mJy	1.100	J2052-3640

Table 1. Summary of target sources and observations

J1639+1127: This quasar sight line is remarkably unique: the quasar sight line pierces through the disc / spiral arm of a nearby galaxy and exhibits signatures of reddening by

dust and the presence of rare diffuse interstellar bands (see Fig. 1). Using GMRT a very strong HI 21-cm absorption (integrated optical depth = 15.70 +/- 0.13 km/s) is detected at the redshift of the galaxy (Srianand et al. 2013, MNRAS, 428, 2198). This absorption feature (presented later in the report) is expected to be detected in the MeerKAT observations at a signal-to-noise ratio > 100.

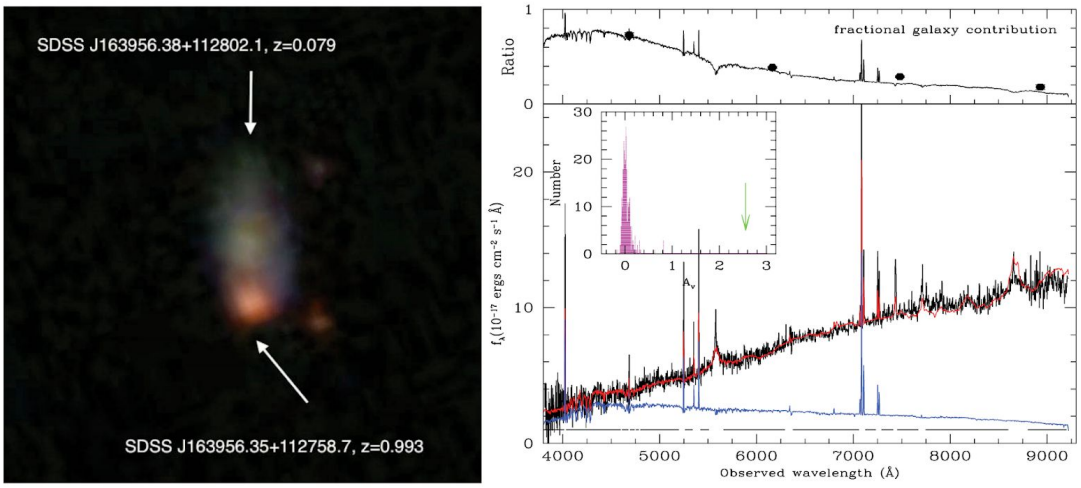

Fig. 1 SDSS colour image (30" x 30") showing the QSO (SDSS J163956.35+112758.7,z_{qso}=0.993) sight line piercing through the disc/spiral-arm of the foreground galaxy (SDSS J163956.35+112802.1,z_{gal}=0.079) Right: the SDSS spectrum of the QSO is fitted with a combination of a reddened QSO composite spectrum and a spiral galaxy template (blue spectrum) from SDSS.

J2023-3655: The target source, also known as PKS2020-370, has a flux density of 436 mJy (based on NVSS) at 1.4 GHz. It is a flat spectrum quasar at the redshift of z_{qso} = 1.1. Carilli et al. (1987, ApJ, 319, 683) and Boisse et al. (1988, A&A, 191, 193) have reported detection of HI 21-cm absorption line towards the quasar at z=0.0287, which corresponds to the redshifted 21-cm line frequency of 1380.78 MHz. The absorbing gas originates from the outer HI disk of a galaxy, Klemola 31A (see Figure 2). In the published VLA spectrum with a spectral resolution of ~10 km/s, the absorption line has a peak optical depth of ~10 mJy. In the optical spectrum of the quasar, absorption lines of CaII are also detected at the same redshift. The galaxy Klemola 31A is part of a six member galaxy group. Several VLA datasets from multiple array configurations are available in the VLA archive. More recently, in 2017 the target has also been observed by the MALS team with MeerKAT-16 array and GMRT. The field is a good target to test the HI absorption and emission line capabilities of MeerKAT. This report focuses only on HI absorption and radio continuum properties of the target.

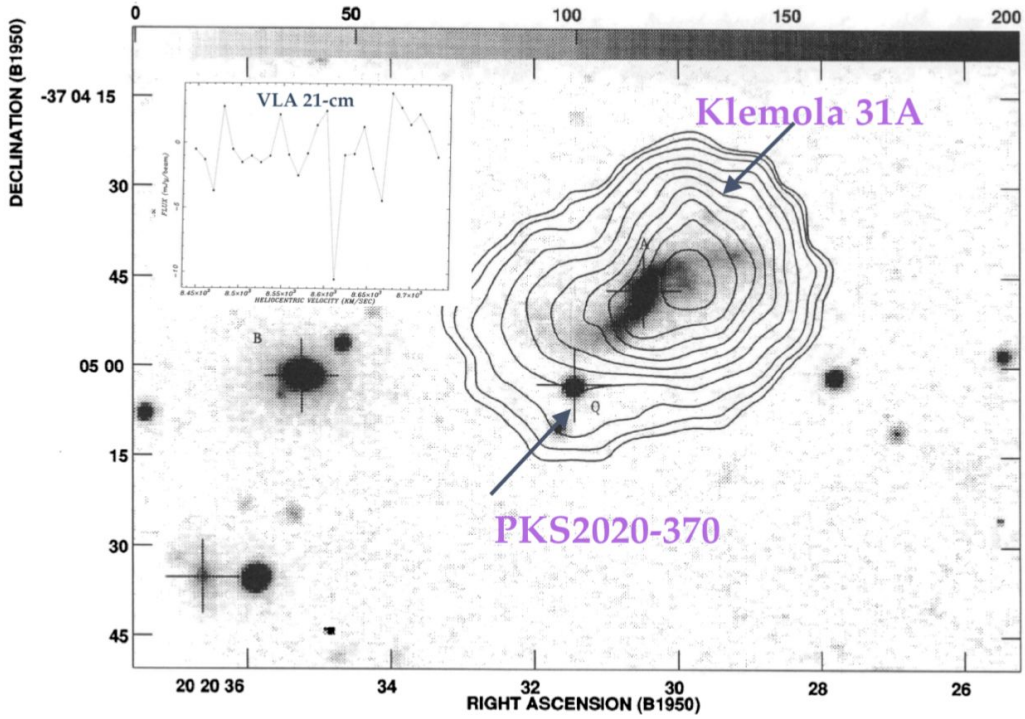

Fig. 2 VLA HI 21-cm line contours overlaid on DSS optical image. The detected HI 21-cm absorption line is also shown.

The full dataset in measurement set format (3.8 TB) was staged at IDIA and then transferred to IUCAA over the internet. The processing was done on the VROOM cluster at IUCAA using the latest version of ARTIP based on CASA 5.6.1 (details at: https://mals.iucaa.in/releases).

2. Data Analysis: flagging and calibration

For this report we are interested only in stokes-I properties, so we generated a measurement set with only XX and YY polarization products and frequency channels 512 - 31230. This measurement set with 30720 frequency channels was processed using ARTIP following exactly the same procedures as described in the report on PKS1830-211. After calibration and flagging through ARTIP-CAL, the continuum imaging performed using ARTIP-CONT (Section 3) and spectral line imaging using ARTIP-CUBE (Section 4).

3. Wideband radio continuum image

The ARTIP-CONT first creates a dataset suitable for continuum imaging. At this step, the data were averaged in frequency per 32 channels (~0.8 MHz) and a more stringent

RFI mask to completely exclude band edges and RFI-affected regions was applied. The frequency range considered for continuum imaging is frequency averaged to 960 channels that were regridded along the frequency axis to obtain a measurement set with 16 physically distinct spectral windows.

We created a widefield broad band 6k x 6k continuum image with a pixel size of 2 arcsec, spanning ~3.3 deg using tclean in CASA. The w-projection algorithm was used as the gridding algorithm in combination with Multi-scale Multi-term Multi-frequency synthesis for deconvolution, with nterms = 2 and four pixel scales to model the extended emission. Two rounds of phase-only self-calibration were carried out along with a final round of amplitude and phase self-calibration. Imaging masks were appropriately adjusted between major cycles during imaging and self-calibration.

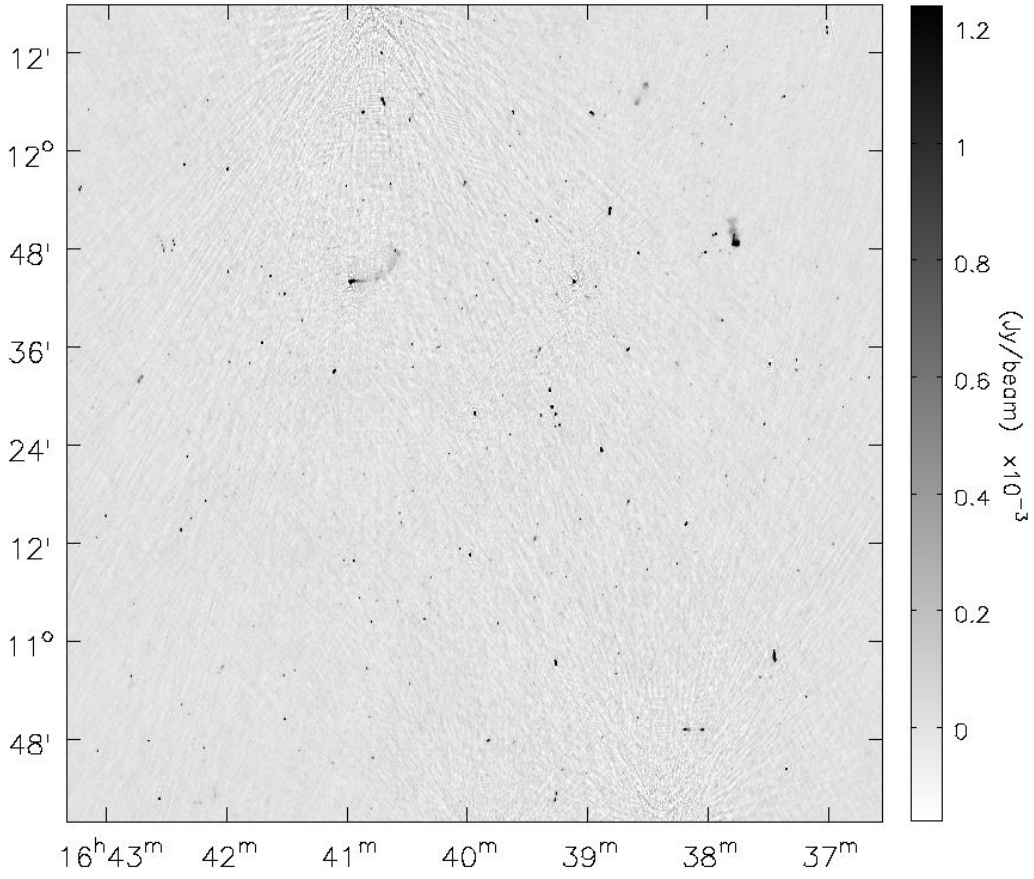

Fig. 3 A portion of the larger 3.3 deg image of J1639+1127 (robust=0; no primary beam correction). The image sensitivity is 15 microJy. The synthesized beam is: 10.8" x 6.9" (position angle = -0.1°).

The final image of source J1639+1127 is shown above, and has an imaging dynamic range of ~11000 made with robust weighting (robust=0) leading to a RMS sensitivity of ~15μJy. There are multiple bright sources located far enough from the phase centre to limit our imaging in the absence of direction dependent corrections. We are in the process of testing direction dependent corrections as a part of the continuum imaging pipeline and will report on it in the future.

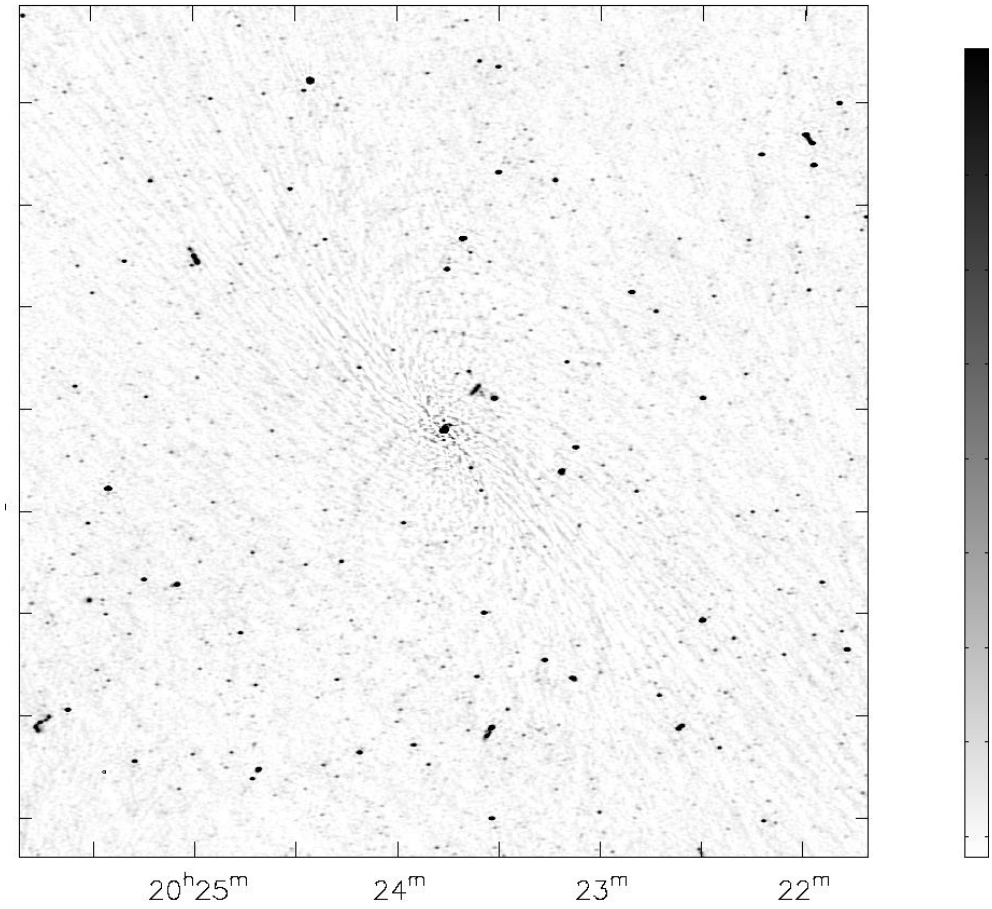

Fig. 4 A portion of the larger 3.3 deg image of J2023-3655 (robust=0; no primary beam correction). The image sensitivity is 9.5 microJy. The synthesized beam is: 12.0" x 7.6" (position angle = +89.2°).

The central source J2023-3655 shown in the image above also displays artifacts in the NW-SE direction at close to noise. This is primarily due to some residual low level RFI in our data missed by the continuum pipeline. The image has an RMS of ~50 microJy around the central source and ~10 microJy overall. The effective dynamic range around the central source is only about 8000.

4. Full 32K spectrum

For the spectral line processing, the calibrated visibilities were split along the frequency axis to create measurement sets that can be processed independently on the cluster nodes. Specifically, we split 30720 frequency channels into 15 spectral windows. The adjacent spectral windows have an overlap of 256 channels (~7 MHz). The unique frequency ranges covered by these measurement sets are marked as vertical dashed lines in the figures presented here. For easier referencing, we label these as SPW-0 to -14.

The measurement sets for these SPWs were processed for continuum imaging with self-calibration and cube imaging. For continuum imaging, a continuum dataset was generated for each spectral window after averaging 32 channels and excluding RFI-affected frequency ranges. The self-calibration was initiated by predicting model visibilities based on the wideband continuum images obtained in the previous section. Here also two rounds of phase-only and one round of amplitude-and-phase self-calibration were performed.

The self-calibration solutions were then applied to the line dataset. The continuum subtraction was performed using the UVSUB method using CLEAN components obtained in the continuum imaging step described in the previous para. The continuum subtracted visibilities were then inverted to obtain the XX and YY spectral line cubes.

The full spectral resolution L-band stokes-I spectrum after removing the residual continuum and combining XX and YY to generate stokes I are shown in Figs. 5 and 6.

We detect HI 21-cm absorption lines towards both the targets. We have uGMRT spectra for both the absorbers. In Fig. 7 and Table 2 we present a comparison of these with the profiles detected in our MeerKAT spectrum. The profiles are well-matched and the integrated optical depth are also consistently reproduced.

Finally, the spectral rms in the MeerKAT spectra (Robust=2) are consistent (or slightly better) with respect to the theoretically expected value. In the Robust=2 spectrum of J2020-3070 (not presented here) we also detect HI 21-cm emission from the foreground galaxy.

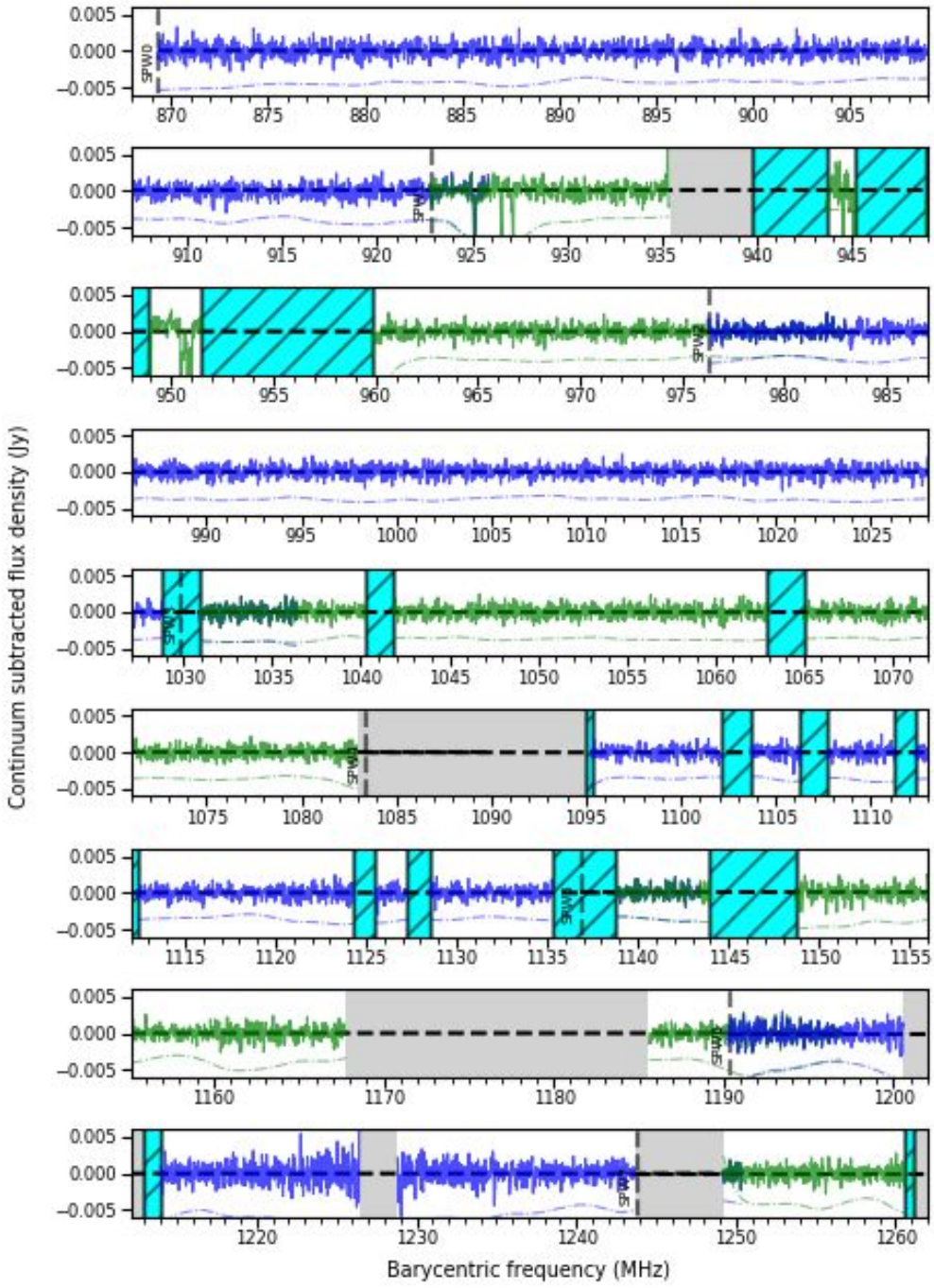

Fig. 5 L-band spectrum of J1639+1127. Shaded region corresponds to the initial RFI mask applied at the start of processing. Hatched regions (corresponding to RFI spikes) were rejected after CUBE-imaging. Vertical dashed lines mark edges of SPW-0 to SPW-14 used to parallelize ARTIP-CUBE processing. The spectra from adjacent SPWs are plotted alternately in blue and green. The adjacent SPWs overlap by ~7 MHz. The Galactic HI 21-cm line and HI/OH absorption towards the quasar are labelled. Dashed-dotted line is the error spectrum (5σ).

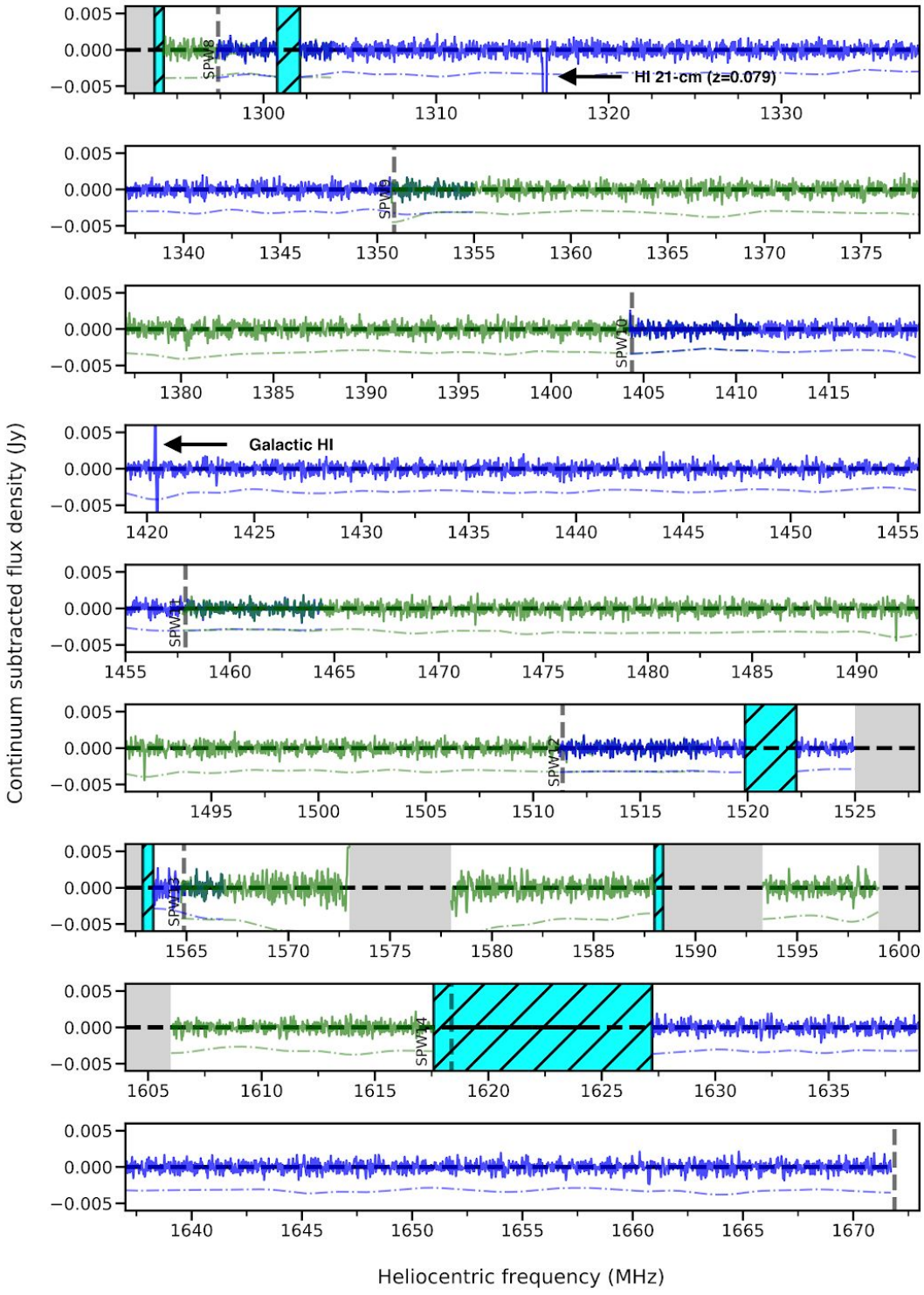

Fig. 5 Continued

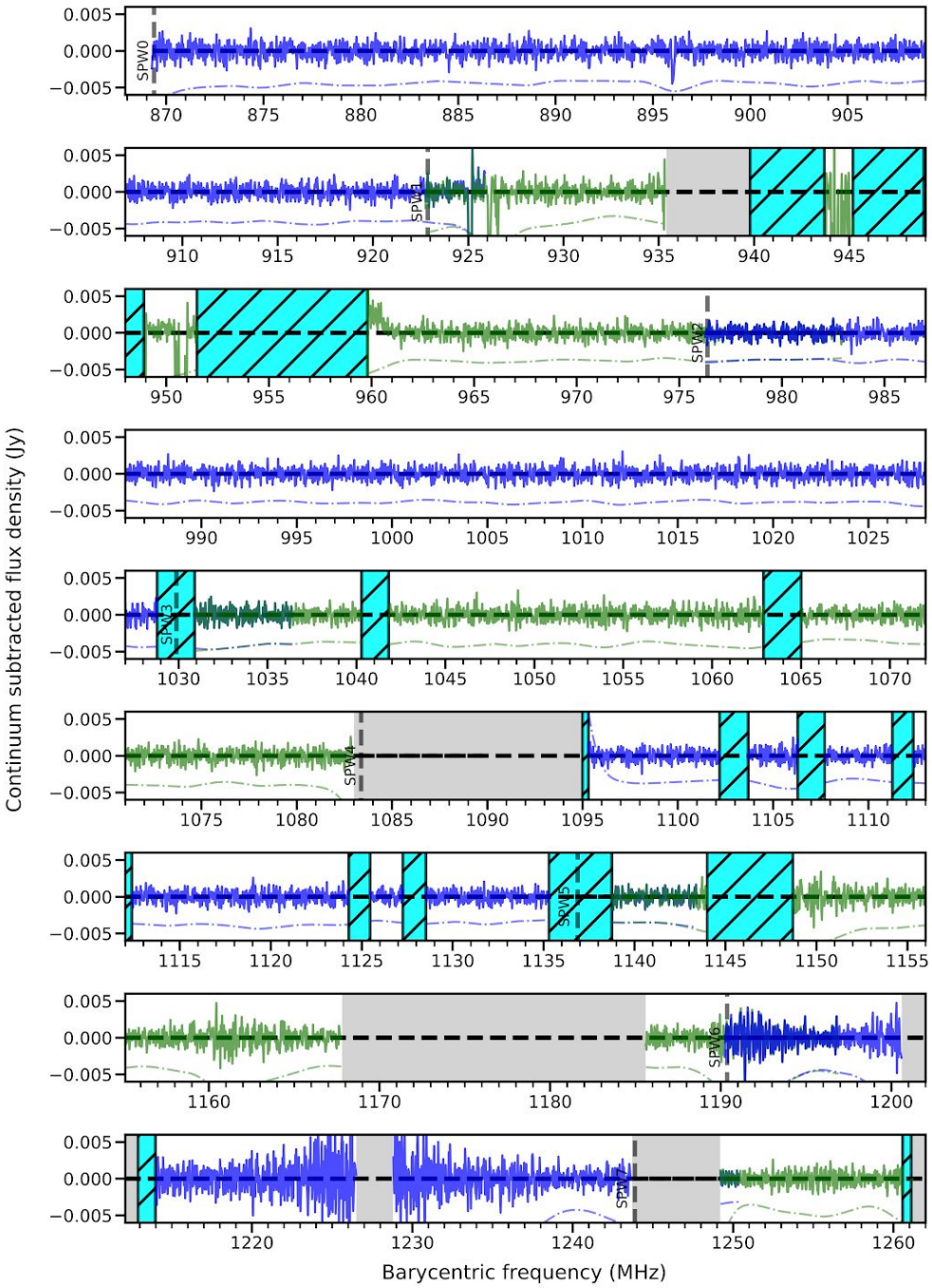

Fig. 6 L-band spectrum of J2023-3655. Shaded region corresponds to the initial RFI mask described in Section 2. The Galactic HI 21-cm line and HI absorption towards the quasar are labelled. All the other details are same as in Fig. 5.

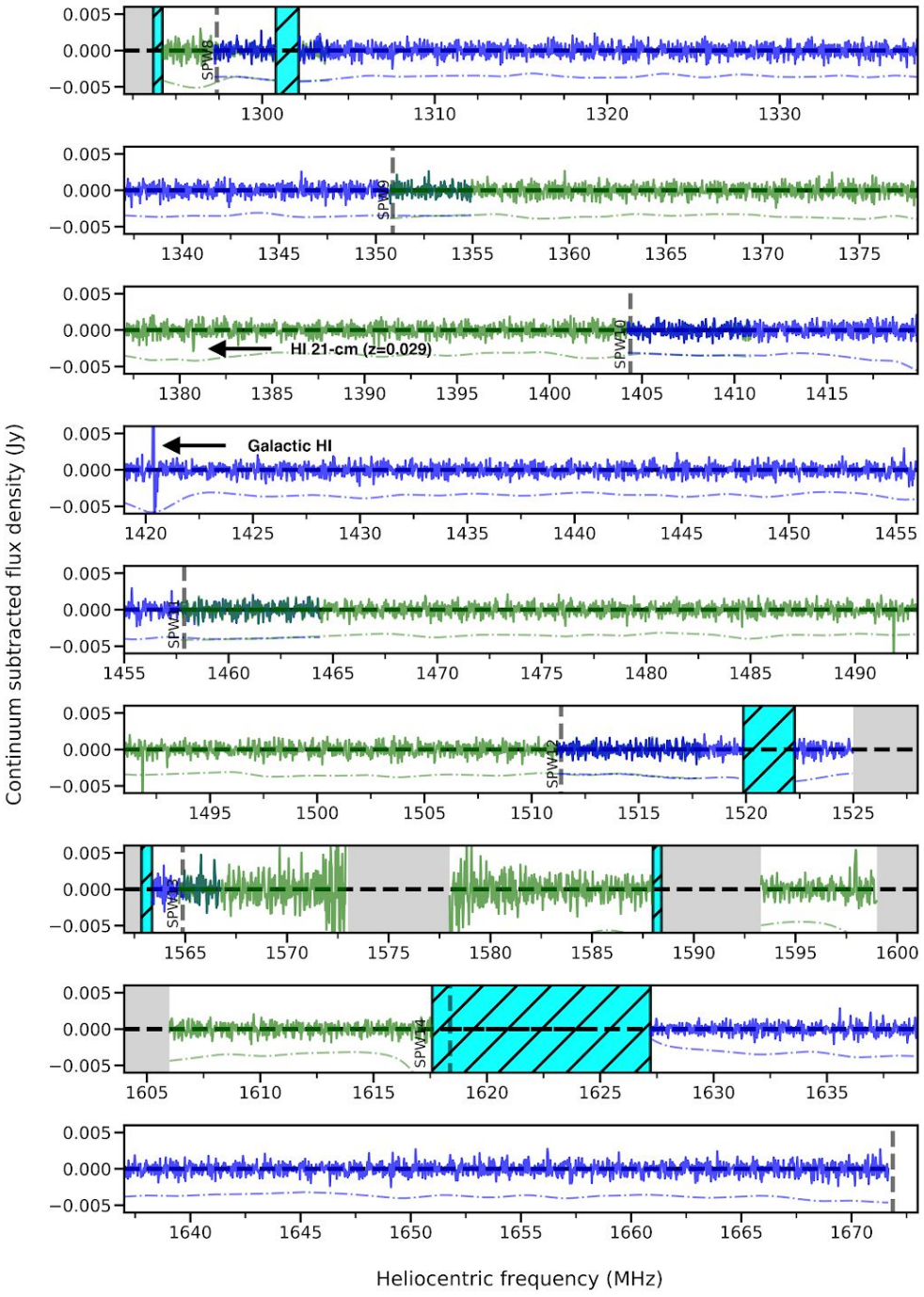

Fig. 6 Continued

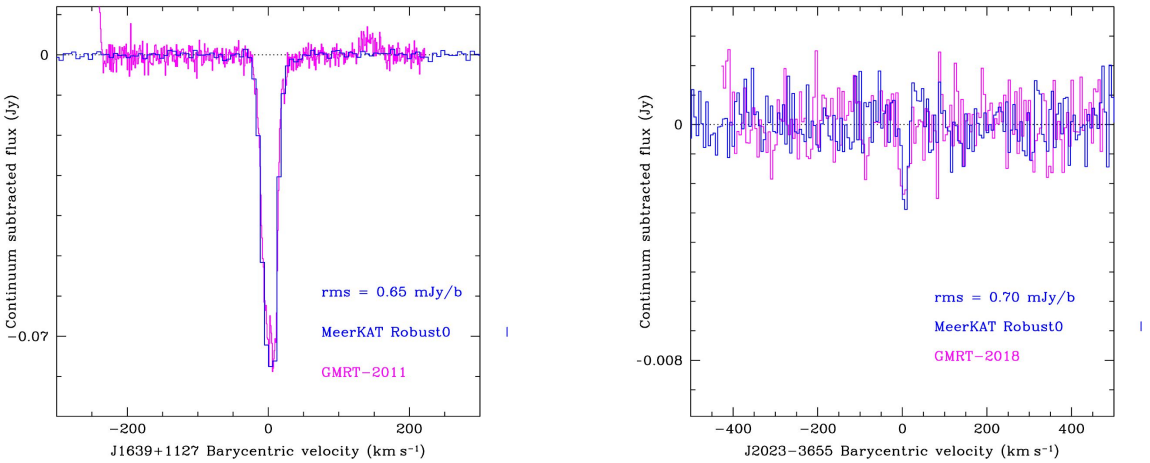

Fig. 7 Comparison of the HI 21-cm absorption profiles detected in the MeerKAT (Robust = 0) and the GMRT spectra of J1639+1127 (Srianand et al. 2013) and J2023-3655 (unpublished). The zero of the velocity scale is centered at z= 0.0791 and z = 0.0287, respectively.

Target	Integrated optical depth (km/s)		Spectral rms in MeerKAT spectra (mJy/beam)*	
	GMRT	MeerKAT	Expected	Measured
J1639+1127	15.70 +/- 0.13	15.75 +/- 0.09	0.59	0.51
J2023-3655	0.11 +/- 0.04	0.09 +/- 0.02	0.59	0.57

* Robust = 2; measured in SPW8 and SPW9.

Table 2. Summary of spectral line results

5. Concluding remarks

The fields centered at J1639+1127 and J2023-3655 were observed on April 1, 2020 with MeerKAT-64 array using 59 antennas. The data were processed using ARTIP on the VROOM cluster at IUCAA. The radio continuum properties of the source are consistent with the published results. We detect known HI 21-cm absorbers towards both the targets. The absorption line properties are consistent with profiles obtained with the GMRT. The spectral rms in the MeerKAT spectra are consistent or slightly better with respect to the theoretically expected value. We also achieve near theoretical sensitivities using the automated continuum calibration and imaging pipelines. Work is underway to incorporate direction dependent imaging corrections to the ARTIP-CONT pipelines and we will revisit low level RFI flagging on a case by case basis.